Stability of distribution of F18 flurpiridaz after transient coronary occlusion in pigs

Rudolf A. Werner, Kazuhiro Koshino, Kenji Arimitsu, Constantin Lapa, Mehrbod S. Javadi, Steven P. Rowe, Naoko Nose, Hiroyuki Kimura, Kenji Fukushima, Takahiro Higuchi

Angaben zur Veröffentlichung / Publication details:

Werner, Rudolf A., Kazuhiro Koshino, Kenji Arimitsu, Constantin Lapa, Mehrbod S. Javadi, Steven P. Rowe, Naoko Nose, Hiroyuki Kimura, Kenji Fukushima, and Takahiro Higuchi. 2019. "Stability of distribution of F18 flurpiridaz after transient coronary occlusion in pigs." *JACC: Cardiovascular Imaging* 12 (11, Part 1): 2269–71. https://doi.org/10.1016/j.jcmg.2019.05.018.

Stability of Distribution of F18 Flurpiridaz After Transient Coronary Occlusion in Pigs

Beyond commonly used myocardial perfusion imaging (MPI) radiotracers compatible with single-photon emission computed tomography (SPECT) imaging, positron emission tomography (PET) agents offer several key advantages. Nonetheless, the short half-life of clinically used PET MPI radiotracers limits a more widespread adoption into clinical practice. However, novel F18-labeled MPI agents (half-life, 110 min) may allow for more practicality in a busy PET practice (1). Notably, the novel PET MPI radiotracer F18 flurpiridaz has demonstrated high first-pass extraction (>90%), potentially rendering F18 flurpiridaz an ideal PET radiotracer to assess myocardial blood flow (2).

Current commercially available MPI SPECT radiotracers recommend an injection of the radiopharmaceutical during peak exercise along with radiotracer-specific waiting times prior to image acquisition (3). However, for F18 flurpiridaz, the distribution-redistribution pattern along with the optimal imaging time is not yet fully elucidated. We aimed to assess the stability of myocardial F18

FIGURE 1 **F18 Flurpiridaz in P-O and O-R Pig Models**

A

Time after Tracer IV (min)	Controls	Permanent-Occlusion (SUV)			Occlusion-Reperfusion (SUV)		
		Defect (D)	Remote (R)	D-R-Ratio	Defect (D)	Remote (R)	D-R-Ratio
5-10	8.0 ± 1.2	2.7 ± 1.3	5.6 ± 2.6	0.36 ± 0.21	2.5 ± 0.6	8.4 ± 2.6	0.39 ± 0.05
10-15	8.7 ± 1.4	2.8 ± 1.3	6.2 ± 2.9	0.34 ± 0.20	2.9 ± 0.7	9.3 ± 2.7	0.40 ± 0.06
15-30	9.6 ± 1.7	3.1 ± 1.4	6.7 ± 3.1	0.35 ± 0.20	3.3 ± 0.9	9.8 ± 2.9	0.43 ± 0.05
30-60	10.5 ± 1.9	3.2 ± 1.5	7.1 ± 3.2	0.34 ± 0.20	3.9 ± 1.0	10.6 ± 3.0	0.47 ± 0.05
60-90	10.6 ± 2.2	3.2 ± 1.4	7.2 ± 3.2	0.34 ± 0.19	4.1 ± 0.9	10.4 ± 2.6	0.50 ± 0.06
90-120	10.2 ± 2.0	3.1 ± 1.4	7.2 ± 3.2	0.32 ± 0.19	4.0 ± 0.6	10.0 ± 2.2	0.51 ± 0.07

B

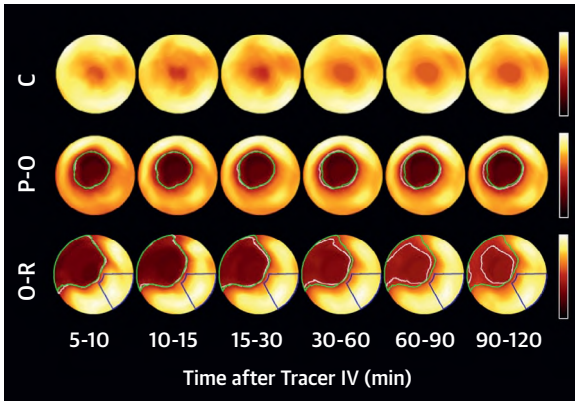

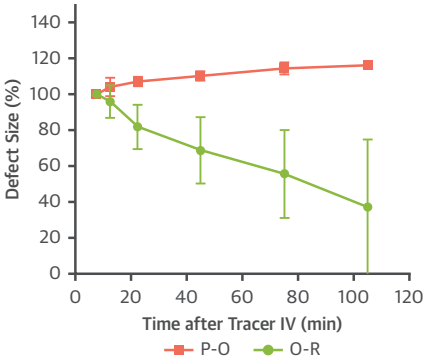

C

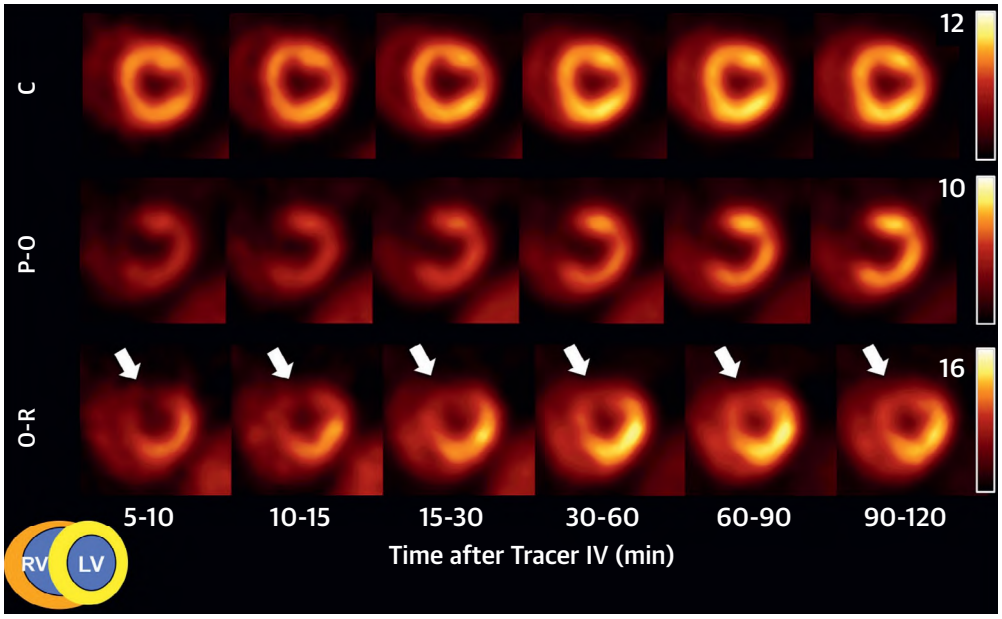

(A) SUVs for C and remote regions/defect areas of the P-O and the O-R models (mean ± SD). **(B) (Left)** Myocardial polar maps for C, P-O, and O-R. In polar maps of both occlusion models, **white lines** indicate boundaries between normal and defect regions at each time point, whereas **green lines** show the boundaries of those regions at 5 to 10 min after radiotracer injection. Reference regions are given in **blue. (Right)** Defect size in percentages for both coronary occlusion models (P-O vs. O-R, mean ± SD). **(C)** Representative serial short axis images of in vivo pig cardiac PET imaging for each group (C vs. P-O vs. O-R). For the P-O model, the defect remains almost stable throughout the imaging session, whereas for the O-R model, a reduction of the defect size over time is indicated (**white arrows**). Color bars are labeled with SUV. C = controls; D-R = defect-remote; IV = intravenous; LV = left ventricle; O-R = occlusion-reperfusion; P-O = permanent-occlusion; PET = positron emission tomography; R = remote; SUV = standardized uptake values.

flurpiridaz distribution in a pig model of transient coronary occlusion mimicking the clinical setting of a stress perfusion protocol.

The following pig models were evaluated: healthy controls (n = 4), a permanent occlusion model (permanent mid left descending artery [LA]) occlusion, n = 3), and an occlusion-reperfusion model (n = 4, tracer administration at the start of the occlusion and release of the snare after 2-min occlusion).

Controls demonstrated homogenous uptake throughout the left ventricular (LV) myocardium over the imaging session of 2 h. In both coronary occlusion models, a clear radiotracer uptake defect in the distal anteroseptal wall was found. For the permanent occlusion model, the uptake defect remained stable with the following defect areas in percentages (normalized at 8 min): 13 min, 104 ± 4%; 23 min, 107 ± 1%; 45 min, 110 ± 2%; 75 min, 114 ± 3%; and 105 min, 116 ± 3% LV (averaged slope, 0.12 ± 0.10%/min). For the occlusion-reperfusion model, the following percentage defect areas were derived (normalized at 8 min): 13 min, 96 ± 8%; 23 min, 82 ± 11%; 45 min, 68 ± 16%; 75 min, 56 ± 21%; and 105 min, 37 ± 32% LV (averaged slope −0.62 ± 0.19%/min, $p < 0.05$ vs. permanent occlusion) (**Figure 1**). Blood clearance was determined by drawing a region of interest in the LV cavity by carefully avoiding myocardial spill-over. Retention indices (%/min, myocardial standardized uptake values [SUV] at time *t* divided by integral of LV cavity SUV to 3 min) were as follows: permanent occlusion (8 min, 24 ± 11; 13 min, 25 ± 11; 23 min, 27 ± 12; 45 min, 29 ± 13; 75 min, 28 ± 13; and 105 min, 28 ± 12) versus occlusion-reperfusion (8 min, 25 ± 6; 13 min, 28 ± 6; 23 min, 32 ± 8; 45 min, 38 ± 9; 75 min, 39 ± 8; and 105 min, 38 ± 5; $p < 0.001$ vs. remote, respectively).

In summary, the radiotracer uptake defect remained stable over time in the permanent occlusion model, whereas in an occlusion-reperfusion model, a continuous decrease in defect size throughout the 2-h imaging session was noted. Thus, in a clinical setting, these findings may emphasize the need for an early imaging protocol in a stress study. Moreover, the observed results may also suggest that viability assessments using a single F18 flurpiridaz injection are feasible (3,4). However, further research is warranted, e.g., to determine the impact of different durations of ischemia on F18 flurpiridaz distribution-redistribution patterns (5) and to further investigate an increase in SUV, not only in the defect area of the occlusion-reperfusion model, but also to a lesser extent in remote myocardium.

Rudolf A. Werner, MD†
Kazuhiro Koshino, PhD†
Kenji Arimitsu, PhD†
Constantin Lapa, MD
Mehrbod S. Javadi, MD
Steven P. Rowe, MD, PhD
Naoko Nose, BSc
Hiroyuki Kimura, PhD
Kenji Fukushima, MD
Takahiro Higuchi, MD, PhD*

*Department of Nuclear Medicine
Comprehensive Heart Failure Center
University Hospital Würzburg
Oberdürrbacherstr. 6
97080 Würzburg
Germany
E-mail: thiguchi@me.com

https://doi.org/10.1016/j.jcmg.2019.05.018

Please note: †Drs. Werner, Koshino, and Arimitsu contributed equally to this work. This work was supported by the Competence Network of Heart Failure funded by the Integrated Research and Treatment Center (IFB) of the Federal Ministry of Education and Research (BMBF) and the German Research Council (PRACTIS, DFG grant HI 1789/3-3). This work was supported by Grants-in-Aid for Scientific Research (Kakenhi, 15K21774) from the Japan Society for the Promotion of Science (JSPS). This project has received funding from the European Union's Horizon 2020 research and innovation program under the Marie Sklodowska-Curie grant agreement number 701983. The authors have reported that they have no relationships relevant to the contents of this paper to disclose.

REFERENCES

1. Werner RA, Chen X, Rowe SP, Lapa C, Javadi MS, Higuchi T. Moving into the next era of PET myocardial perfusion imaging: introduction of novel (18)F-labeled tracers. Int J Cardiovasc Imaging 2019;35:569–77.

2. Huisman MC, Higuchi T, Reder S, et al. Initial characterization of an 18F-labeled myocardial perfusion tracer. J Nucl Med 2008;49:630–6.

3. Henzlova MJ, Duvall WL, Einstein AJ, Travin MI, Verberne HJ. ASNC imaging guidelines for SPECT nuclear cardiology procedures: stress, protocols, and tracers. J Nucl Cardiol 2016;23:606–39.

4. Pohost GM, Zir LM, Moore RH, McKusick KA, Guiney TE, Beller GA. Differentiation of transiently ischemic from infarcted myocardium by serial imaging after a single dose of thallium-201. Circulation 1977;55:294–302.

5. Yu M, Guaraldi MT, Mistry M, et al. BMS-747158-02: a novel PET myocardial perfusion imaging agent. J Nucl Cardiol 2007;14:789–98.